

APPENDIX E – STUDIES ON THE ELIGANT-GN DETECTION ARRAY

The aim of this chapter is to present several simulations results of ELIGANT-GN array. The configuration of the detector array is the one previously presented in section 3.4 (tables 3.4.1 – 3.4.3), namely 34 3x3 inch LaBr₃ detectors placed at 25 cm from target and 62 20x5 cm BC501 detectors placed at 1 m from target.

First simulation aims to produce the time response of neutron detectors. For this, we considered a monochromatic neutron point source of 3 MeV placed in the middle of the array. As was already presented, our GEANT code can write in output file the average time of energy deposition (only when there was an energy deposition into the detector sensitive volume) when a certain particle crossed inside the sensitive volume of the detector or disregarding the particle type. The results are presented in figure E.1, imposing the condition that a gamma ray crossed the border inside BC501 (red), or a neutron (green) or disregarding the nature of the particle.

We can distinguish three time peaks (~ 5 ns, ~ 15 ns and ~ 45 ns), and by analyzing components given by different particles, we can find explanations:

- First peak at ~ 5 ns is produced by gamma rays produced by neutrons in the Pb target (neutron source is placed inside it);
- Second peak at ~ 15 ns is mainly produced by gamma rays produced by neutrons interacting in the LaBr₃ detectors;
- Third peak at ~ 45 ns have two components: the main one is produced directly by neutrons, and the second smaller one is produced by gamma rays produced by neutron interactions in detector housing materials.

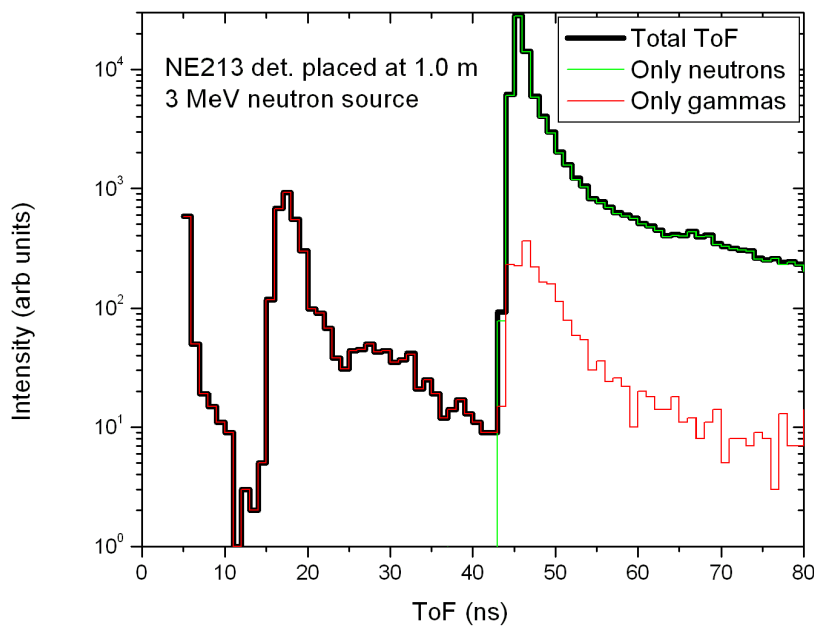


Figure E.1 Time of flight components of NE213 time spectra. Monochromatic point like neutron source.

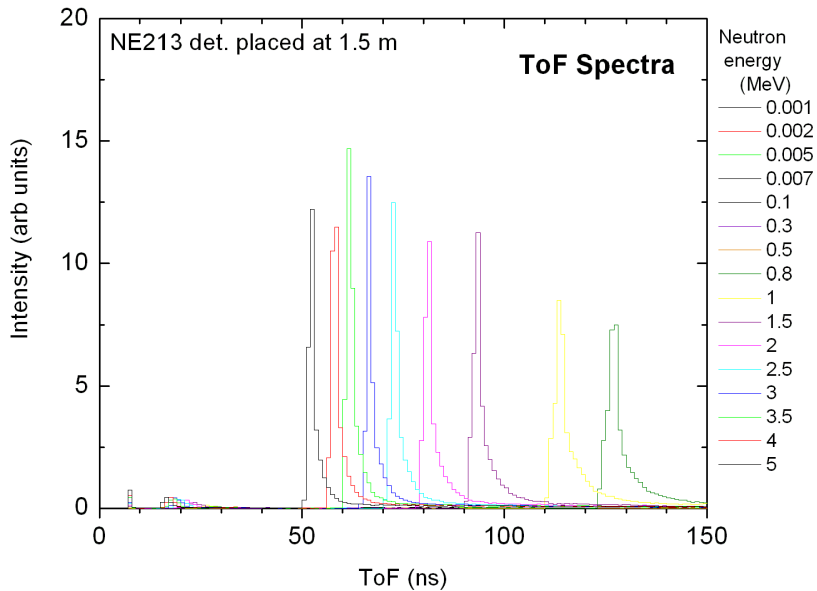


Figure E.2 Time of flight spectra for various neutron energies recorded with NE213 detector array placed at 1.5 m from monochromatic point like neutron source.

In the next figure (E.2) are represented several time spectra for the whole BC501 array considering different neutron emission energies from 1 keV to 5 MeV. The aim of these simulations is to check time resolving power of BC501 array, especially at high neutron energies in the presence of LaBr₃ detectors and taking into account the neutron scatterings in the concrete walls, gamma beam dump, etc. All these neutron scatterings induce long tails in the neutron spectra. In particular, the result presented in figure E.2 was obtained by placing BC501 detectors at 1.5 m.

In order to check the influence of the distance between neutron detectors and the target, we performed two simulations with BC501 detectors placed at 1m and 1.5 m respectively. To check the differences between the two cases, we performed a fast data analysis of the time spectra obtained in the simulations, trying to get a rough estimate of the peak position and FWHM. The results are presented in the figure E.3. In the upper part are represented the ratios of FWHM to the peak positions (relative errors) as function of neutron emission energy, while in the lower part the peak positions are represented as function of neutron emission energy (the error bars are equal with FWHM) for both distances (blue – 1m, red – 1.5 m). We can see in the upper figure that for higher distance we get smaller relative errors that are increasing with neutron energy, and in the lower figure that for 1.5 m distance is obviously much easier to disentangle between neutrons with different energies.

Another important information that we can extract from simulations is the estimation of absolute detection efficiency. In order to extract this information, we should take into account the fact that usually amplitude spectra of a typical BC501 detector have significance above energies ~100 keVee due to noise. In this respect we implemented three different models in order to simulate the light output produced after energy deposition after electron, proton, carbon or alpha interactions. For this reason, we applied 200 keVee cut on the total energy deposit into BC501 detectors, and then integrated the narrow region around peak position of the time spectra to obtain the absolute neutron detection efficiency estimation for the BC501 detector array. The results are presented in figure E.4 for two distances of BC501 detectors from target (1 m and 1.5 m).

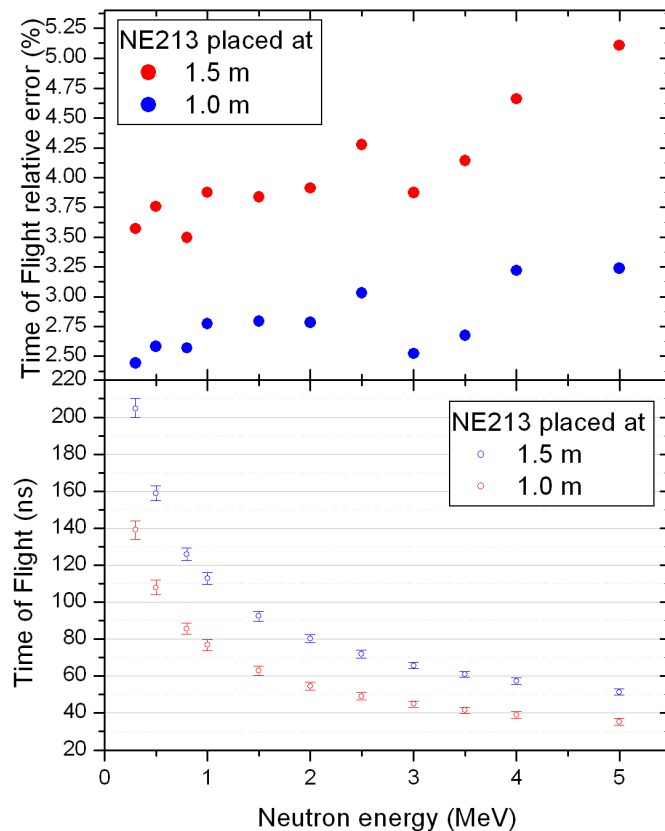


Figure E.3 Time of flight spectra resolution dependence with distance from target for NE213 array.

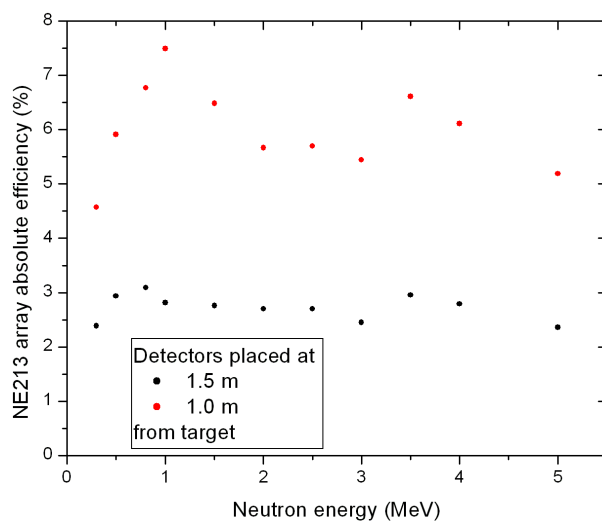


Figure E.4 Absolute detection efficiency of NE213 array. TOF spectra were integrated after a threshold of 200 keVee was applied on total light output spectra.

In figure E.5 is presented the absolute detection efficiency of LaBr₃ array for gamma rays. It was simply obtained by integrating the full energy deposit peak for all 34 LaBr₃ detectors.

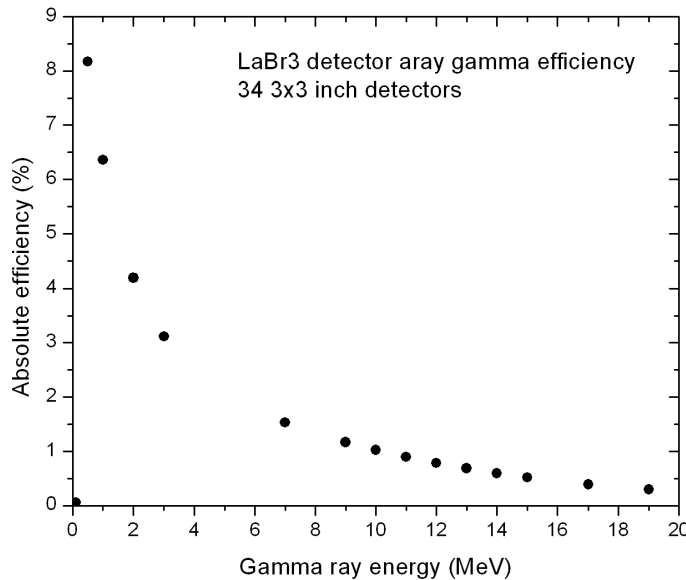


Figure E.5 Absolute detection efficiency of LaBr₃ array.

In the figures below are presented results significant for pile-up study. In all the cases, the experimental hall was filled with air and the detectors were shielded by a set of three attenuators in the following order starting from the surface of the detector: 0.5 mm copper, 0.5 mm cadmium and 1. mm lead. NE213 detectors were placed at 1.5 meters from the target. In all the cases an ideal pencil like gamma ray beam (energy of 8, 13 and 19 MeV) was used.

NE213 response for irradiation of 100 μm Pb target

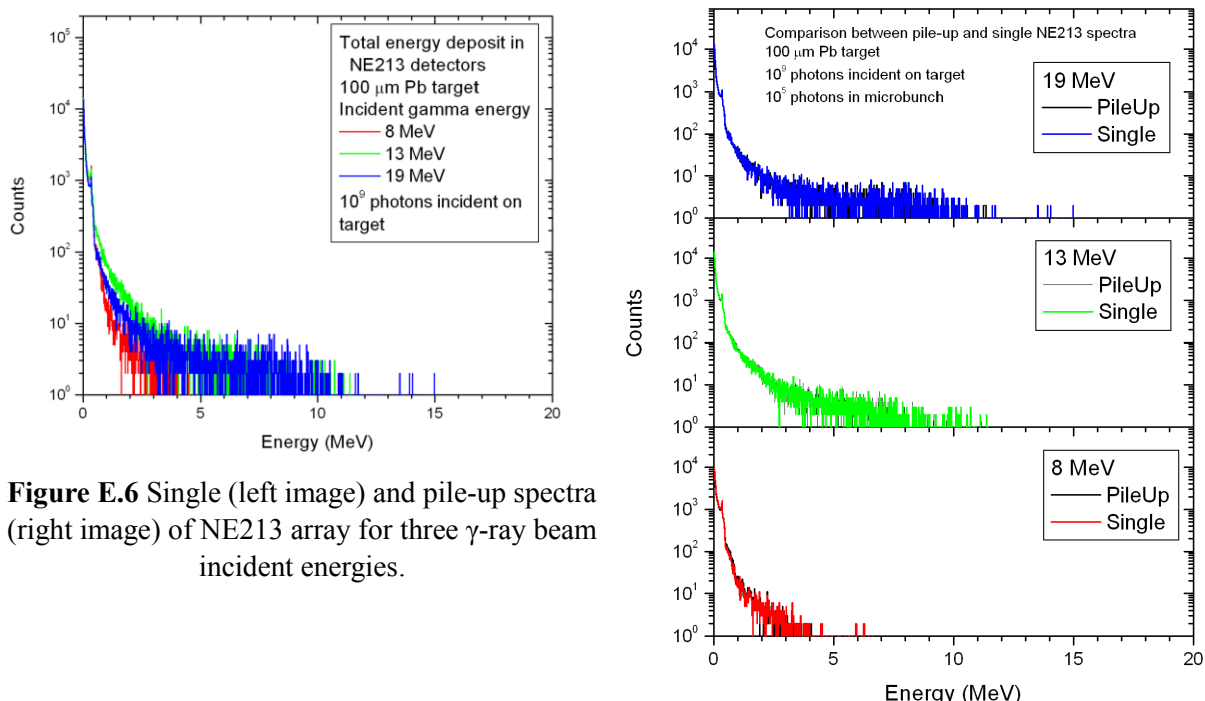


Figure E.6 Single (left image) and pile-up spectra (right image) of NE213 array for three γ -ray beam incident energies.

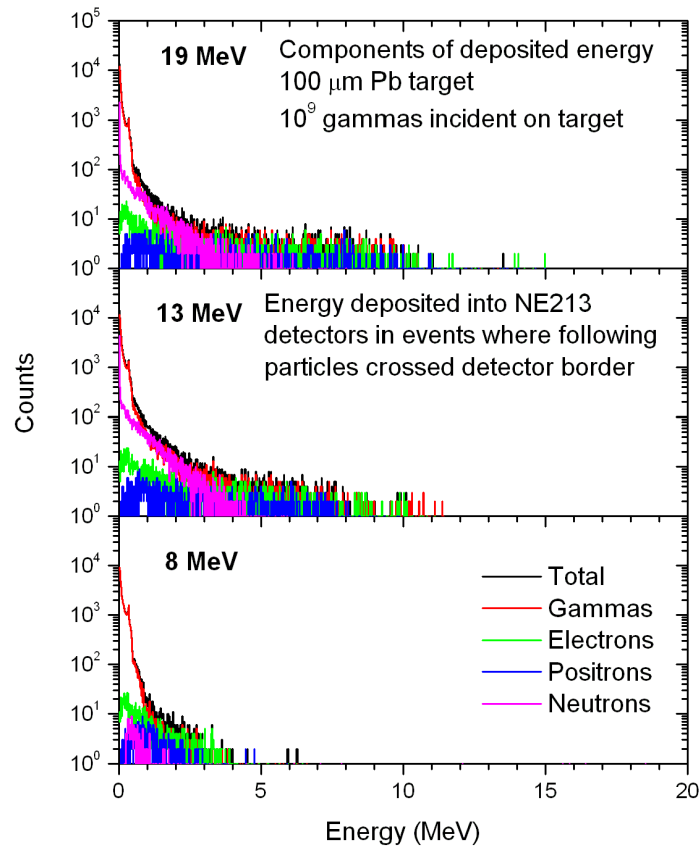


Figure E.7 Components of deposited energy in NE213 detectors for different incident particles.

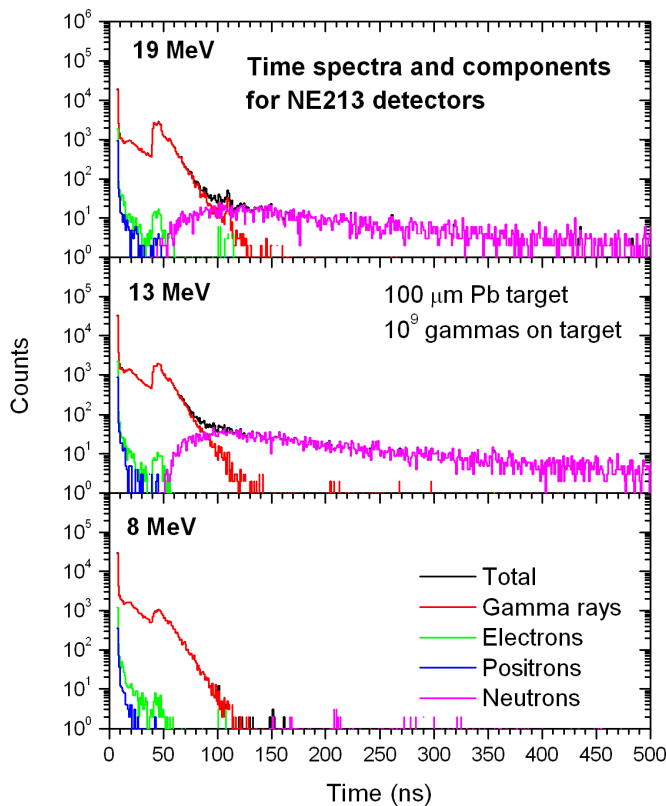
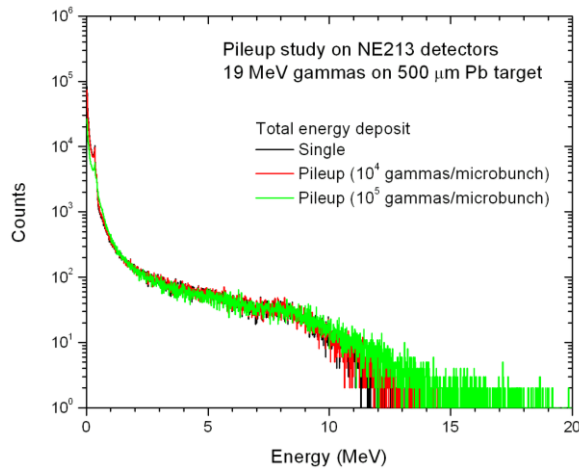
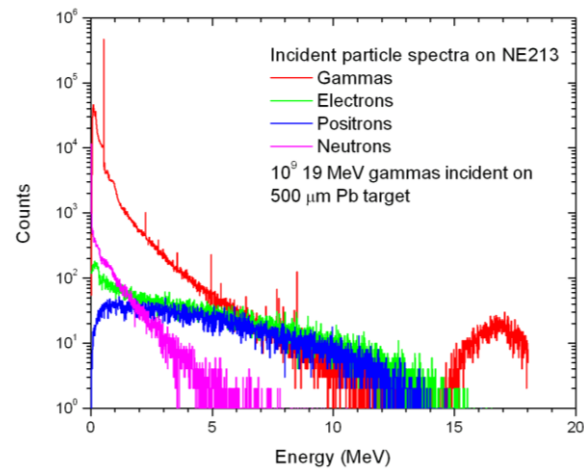
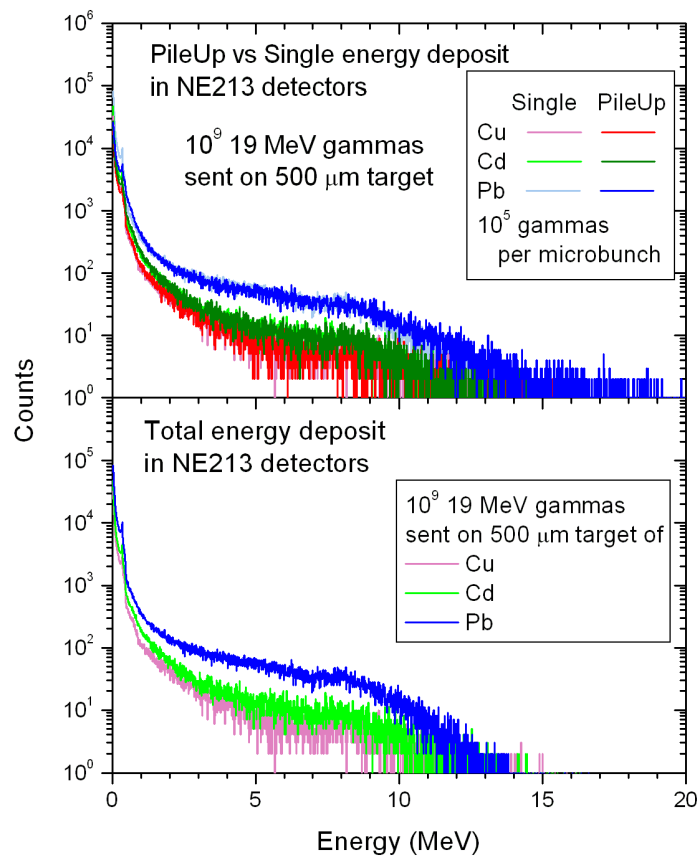


Figure E.8 Components time spectra in NE213 detectors following different incident particles.

NE213 response for irradiation of 500 μm Pb target**Figure E.9** Pile-up spectra in NE213 detectors.**Figure E.10** Energy spectra of incident particles on NE213 detectors.NE213 response dependence with the atomic number of the target**Figure E.11** Pile-up dependence on target atomic number.

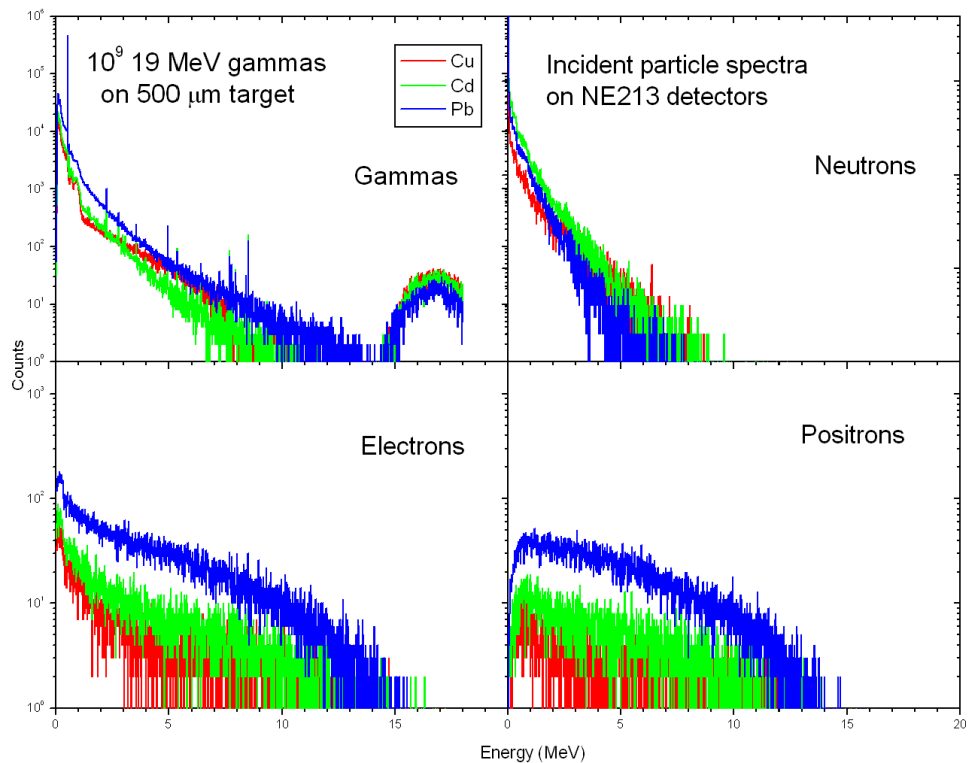


Figure E.12 Dependence of incident particle spectra with target atomic number.

$\text{LaBr}_3:\text{Ce}$ response for irradiation of $100 \mu\text{m}$ Pb target

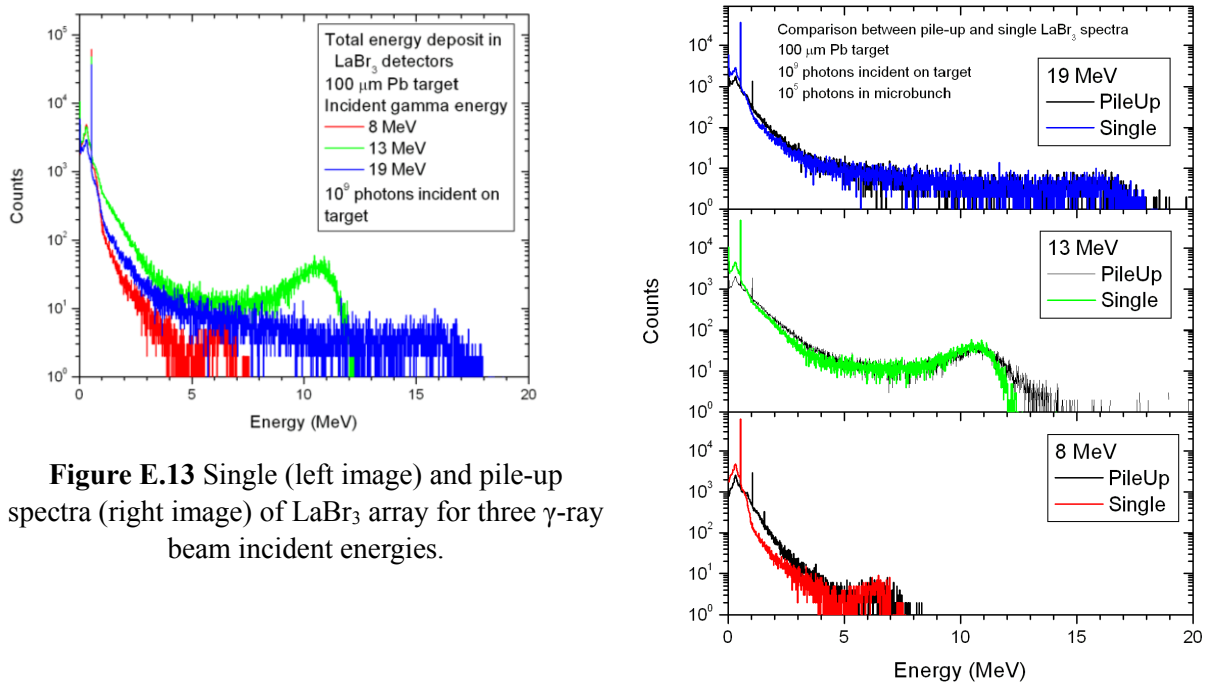


Figure E.13 Single (left image) and pile-up (right image) spectra of LaBr_3 array for three γ -ray beam incident energies.

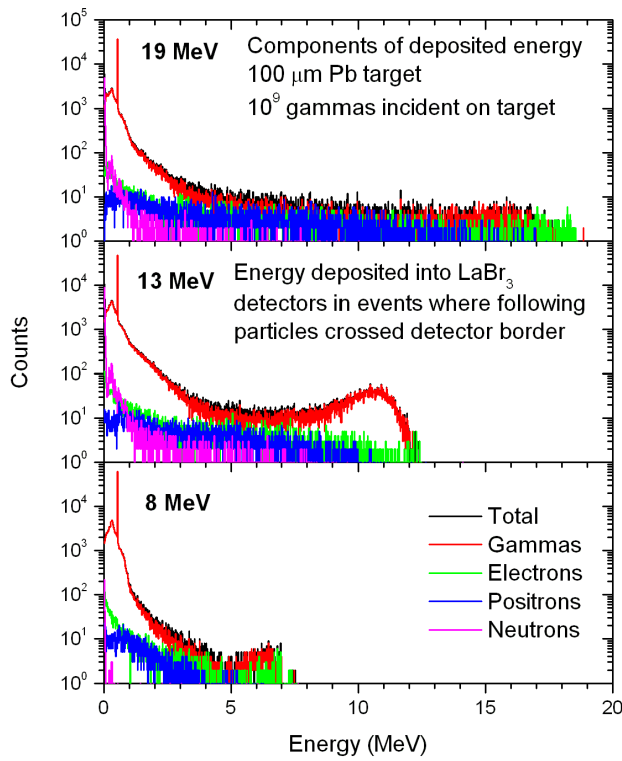


Figure E.14 Components of deposited energy in LaBr_3 detectors for different incident particles.

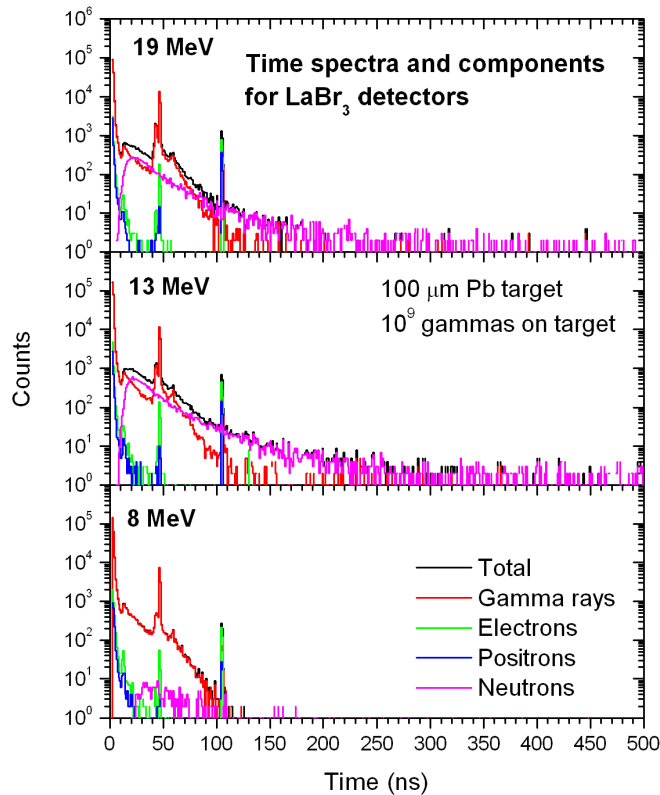
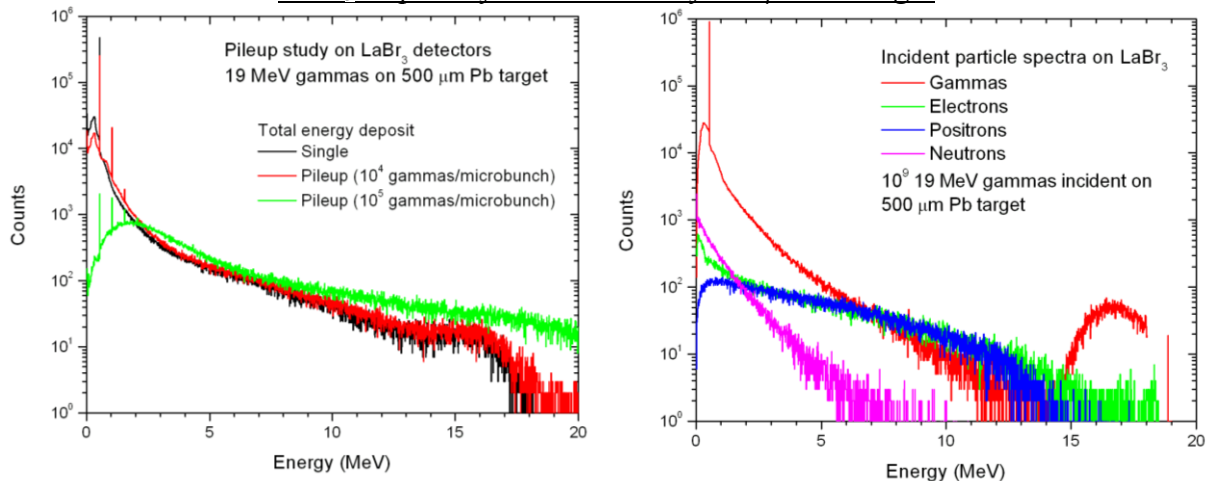
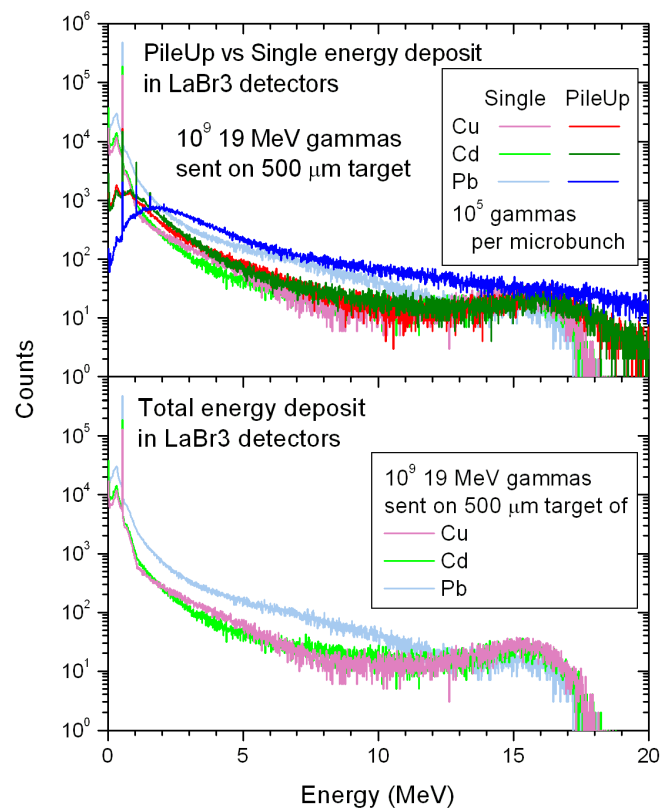


Figure E.15 Components time spectra in LaBr_3 detectors following different incident particles.

LaBr₃ response for irradiation of 500 μm Pb target**Figure E.16** Pile-up spectra in LaBr₃ detectors.**Figure E.17** Energy spectra of incident particles on LaBr₃ detectors.*LaBr₃ response dependence with the atomic number of the target***Figure E.18** Pile-up dependence on target atomic number.

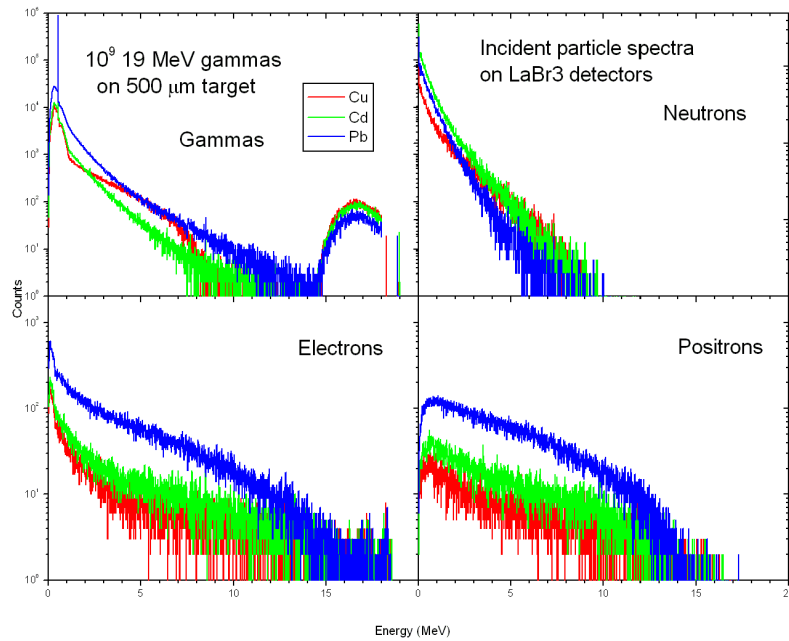


Figure E.19 Dependence of incident particle spectra with target atomic number.

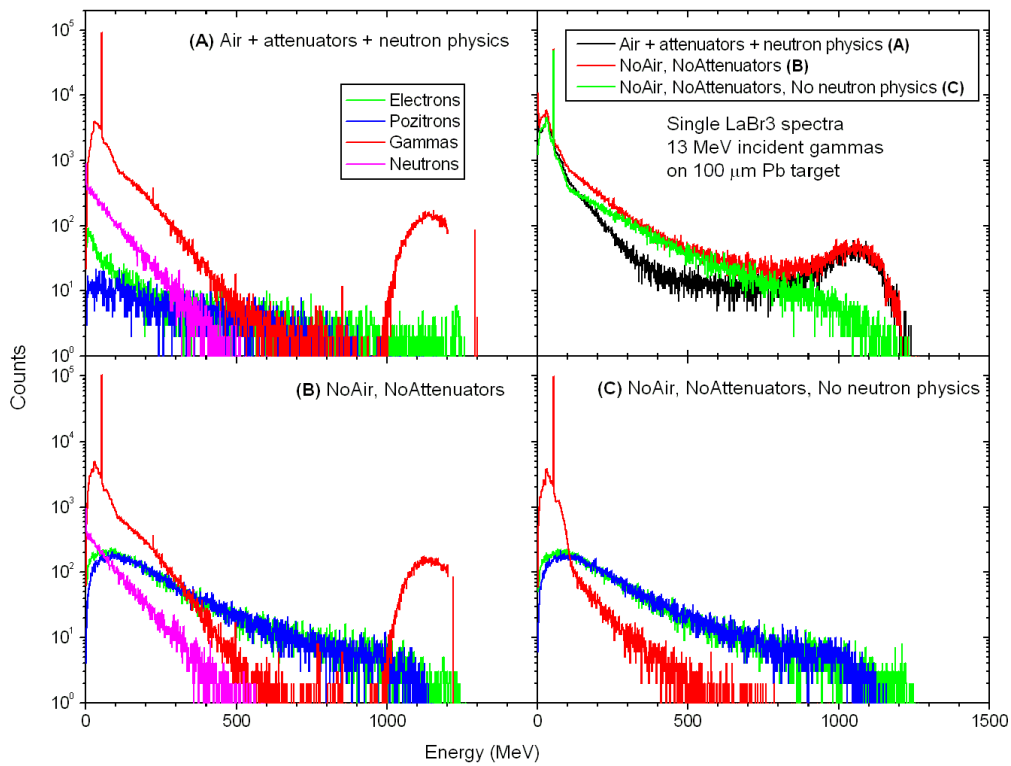


Figure E.20 Dependence of deposited energy and incident particle spectra on LaBr3 detectors in the presence of air in the experimental hall, attenuators in front of detectors. In case (**C**) neutron physics was not considered at all in GEANT simulations.

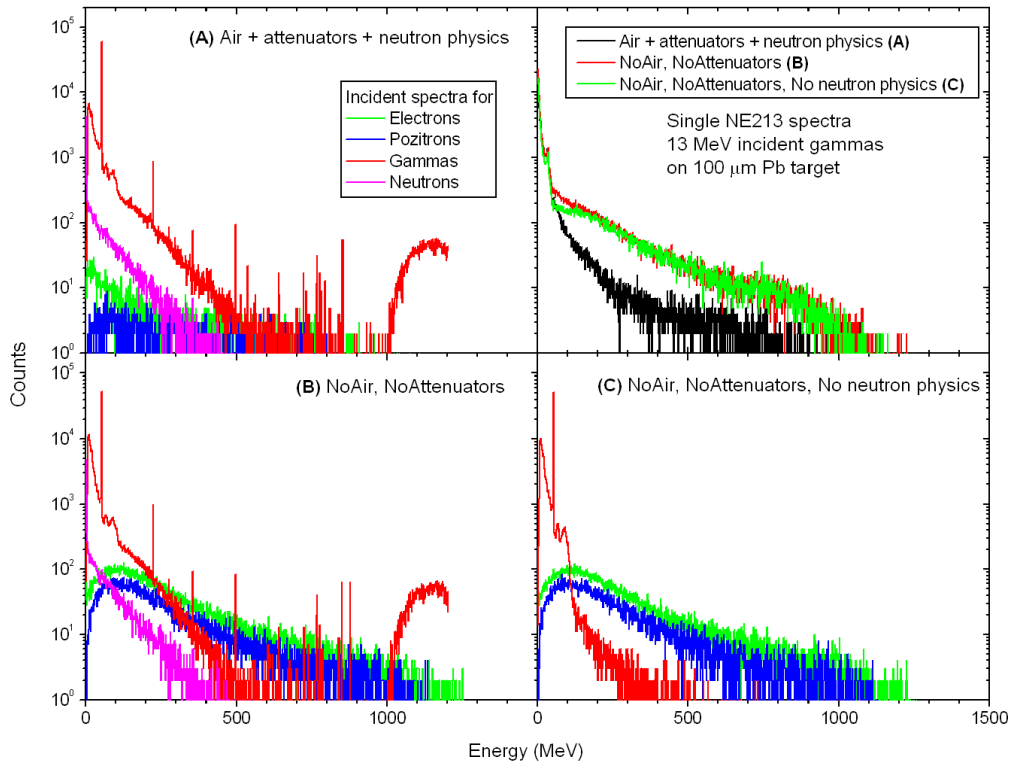


Figure E.21 The same as in Figure E.20 but for NE213 detectors.

